Electronic Supplementary Material (ESI) for Journal of Materials Chemistry C.

Electronic Supplementary Information

Halide-dependent humidity sensing of Cs_2SnX_6 (X = Cl, Br, I) perovskites for real-time human physiological moisture detection

Chen-Chen Guo [a1], Chao-Jie Wang [a1], Le-Xi Zhang [a*], Qi-Da Qiu [a], Meng-Ya Zhu [b], Jing Yin [c], Li-Jian Bie [a*]

[a] School of Materials Science and Engineering, Tianjin Key Lab for Photoelectric Materials and Devices, Key Laboratory of Display Materials and Photoelectric Devices (Ministry of Education), National Demonstration Center for Experimental Function Materials Education, Tianjin University of Technology, Tianjin 300384, China

[b] School of Electronics and Information Engineering, Tianjin Key Laboratory of Electronic Materials and Devices, Hebei University of Technology, Tianjin 300401, China

[c] School of Environmental Science and Safety Engineering, Tianjin University of Technology, Tianjin 300384, China

[*] Corresponding authors:

Le-Xi Zhang, Tel./Fax: +86 022 60214028. E–Mail: lxzhang@tjut.edu.cn.

Li-Jian Bie, Tel./Fax: +86 022 60215508. E–Mail: ljbie@tjut.edu.cn.

[1] These two authors as co-first authors contribute equally to this work.

Section S1. Sensor measurement

All characteristic curves of humidity sensing were measured on a CHS-1 Humidity Sensing Analysis System (Beijing Elite Tech. Co. Ltd. China) at room temperature. The voltage in the humidity test was an alternating current (AC) of 1 V, and the testing frequency varied from 10 Hz to 10^5 Hz. The relative humidity (RH) gradient was achieved at room temperature (~20 °C) using different saturated salt solutions of LiCl (11%), $MgCl_2$ (33%), $Mg(NO_3)_2$ (54%), NaCl (75%), KCl (85%) and K_2SO_4 (97%), respectively.

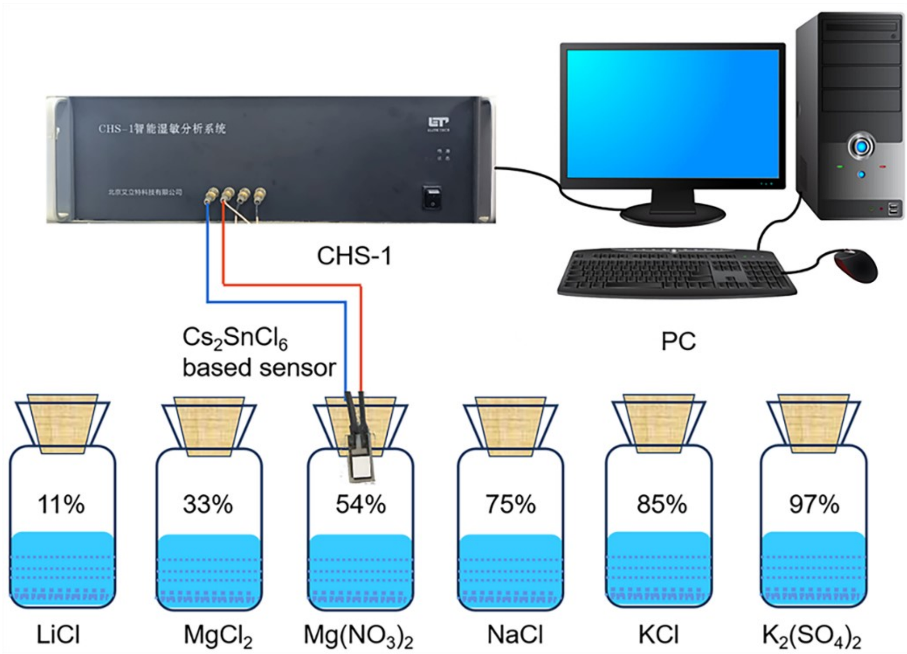

Fig. S1. Flowchart for moisture sensing test.

Section S2. Limit of detection and tolerance factor

The limit of detection (LOD) is calculated by Eq. S1, where y is the response under air humidity, y_i is the average response, N is the number of points, and k is the slope of linear fitting of response at different humidity, respectively.

$$LOD = 3[\sum(y_i-y)^2/N]^{1/2}/k \quad (S1)$$

The tolerance factor (t) of Cs_2SnCl_6, Cs_2SnBr_6 and Cs_2SnI_6 can be calculated by Eq. S2, where r_A, r_B, and r_X correspond to the radii of Cs and Sn cations, as well as Cl, Br and I anions, respectively.

$$t = \frac{(r_A + r_X)}{(\sqrt{2} * (r_B + r_X))} \quad (S2)$$

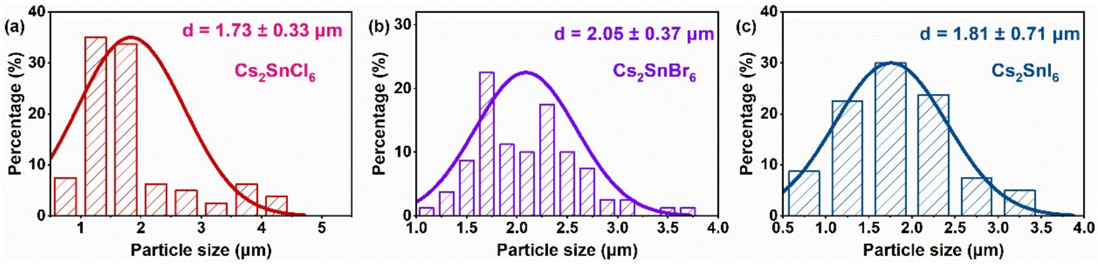

Fig. S2. Particle size distributions of (a) Cs_2SnCl_6, (b) Cs_2SnBr_6 and (c) Cs_2SnI_6, respectively.

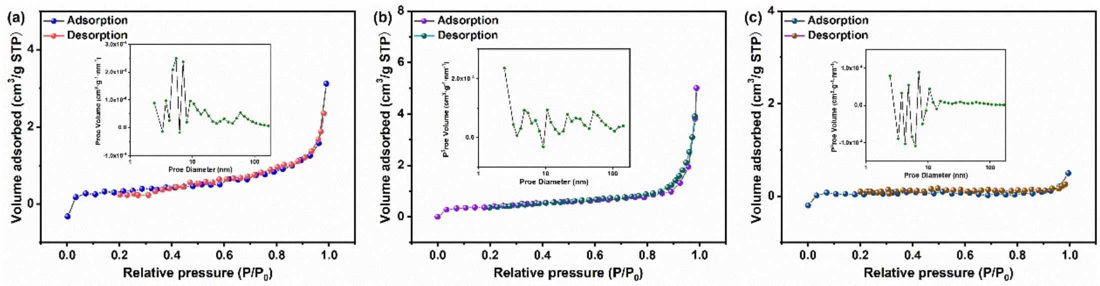

Fig. S3. Typical N_2 absorption-desorption isotherms of (a) Cs_2SnCl_6, (b) Cs_2SnBr_6 and (c) Cs_2SnI_6, respectively. Insets in (a-c): pore size distribution.

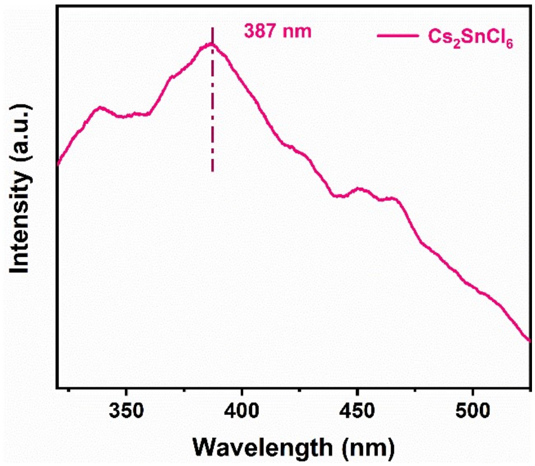

Fig. S4. PL spectrum of Cs_2SnCl_6.

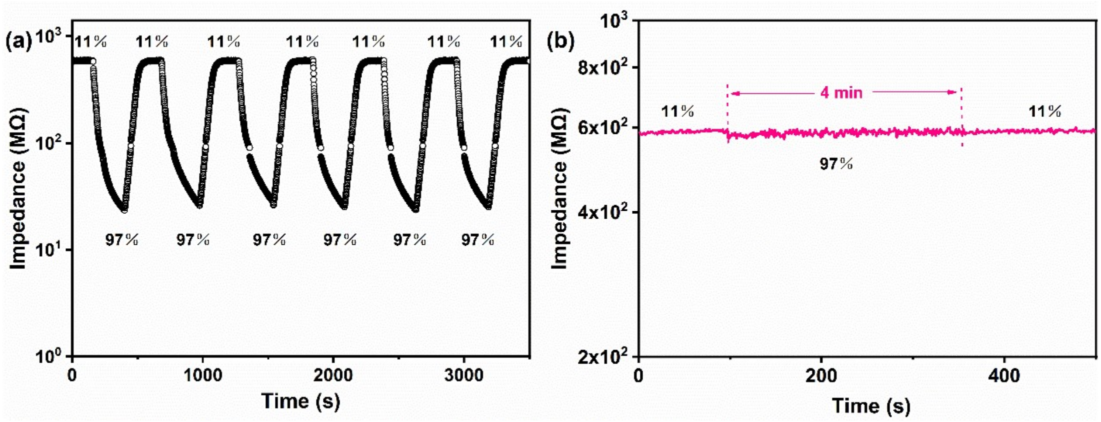

Fig. S5. Real-time impedance changes of (a) a blank Al_2O_3 substrate without a Cs_2SnX_6 layer and (b) the substrate covered with a non-conductive colloidal coating.

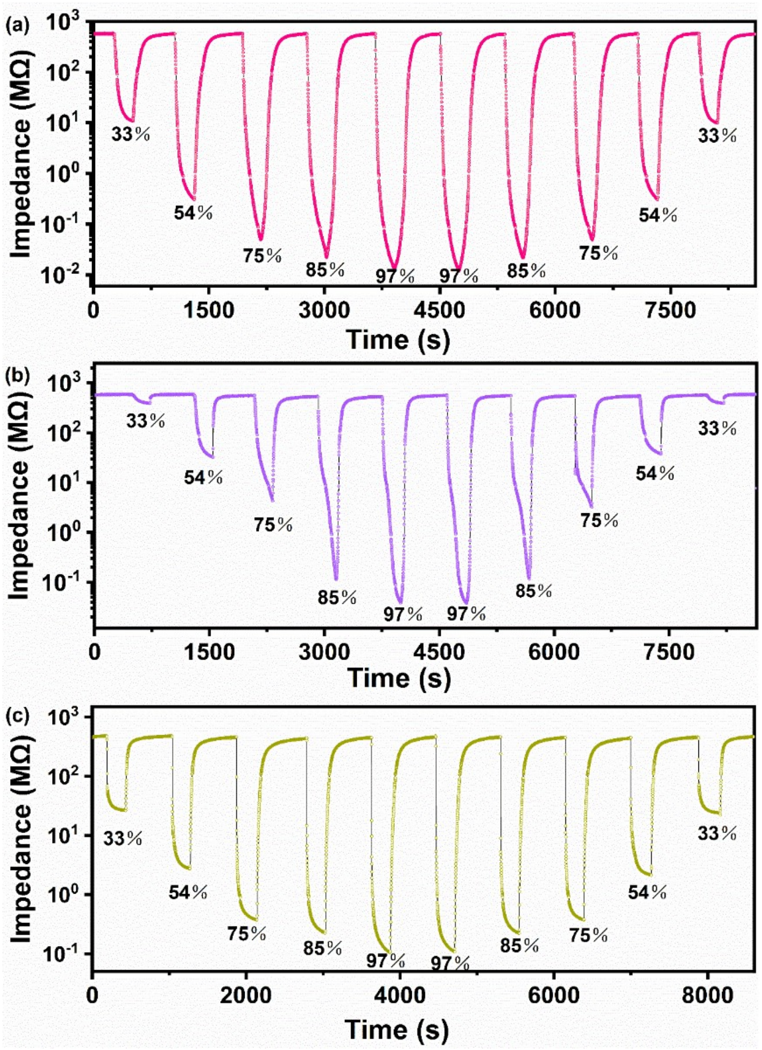

Fig. S6. Dynamic wetting-drying curves of (a) Cs_2SnCl_6, (b) Cs_2SnBr_6 and (c) Cs_2SnI_6, respectively.

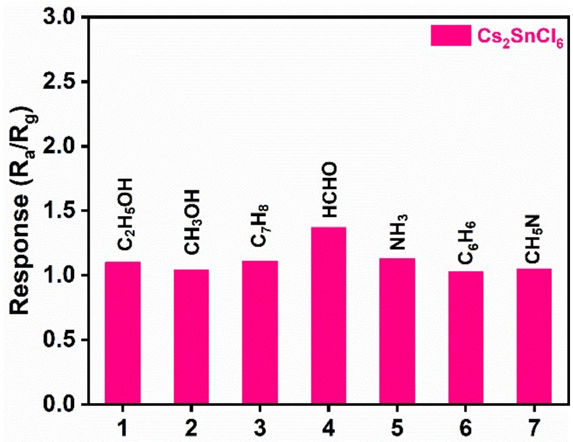

Fig. S7. Response diagram of the Cs_2SnCl_6 sensor to 200 ppm different gases at room temperature.

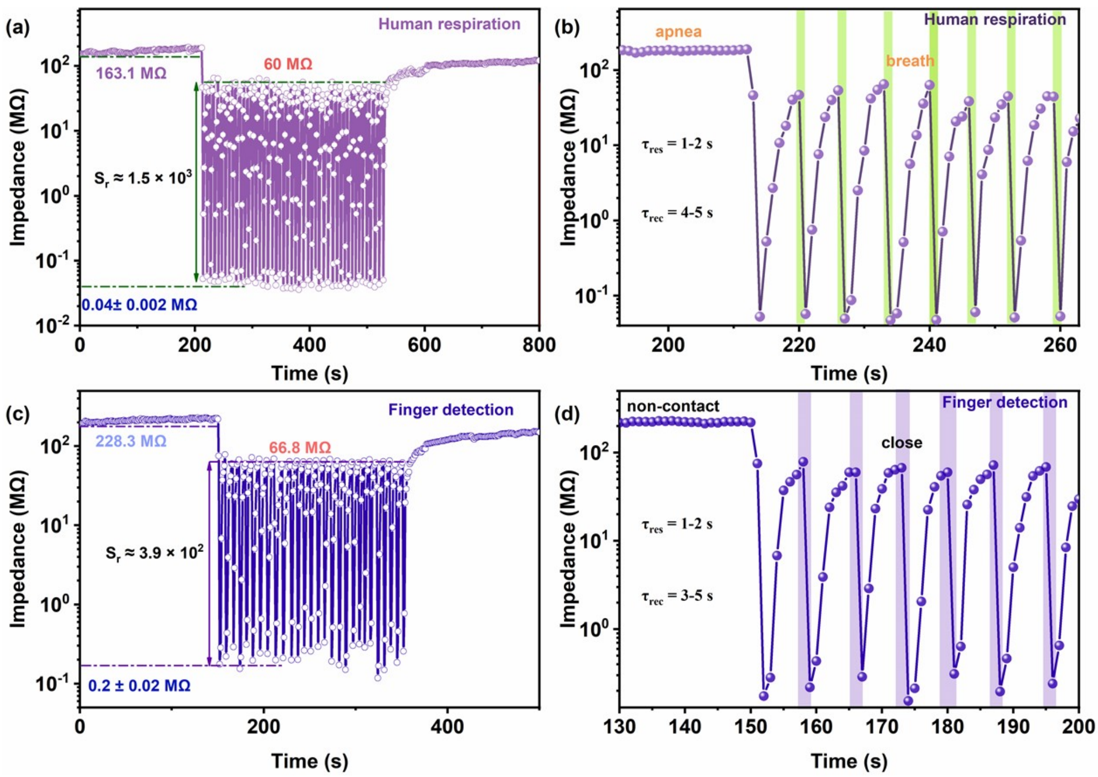

Fig. S8. The dynamic impedance and enlarged curves of monitoring (a, b) human respiration and (c, d) water evaporation from the finger using the Cs_2SnBr_6 sensor.

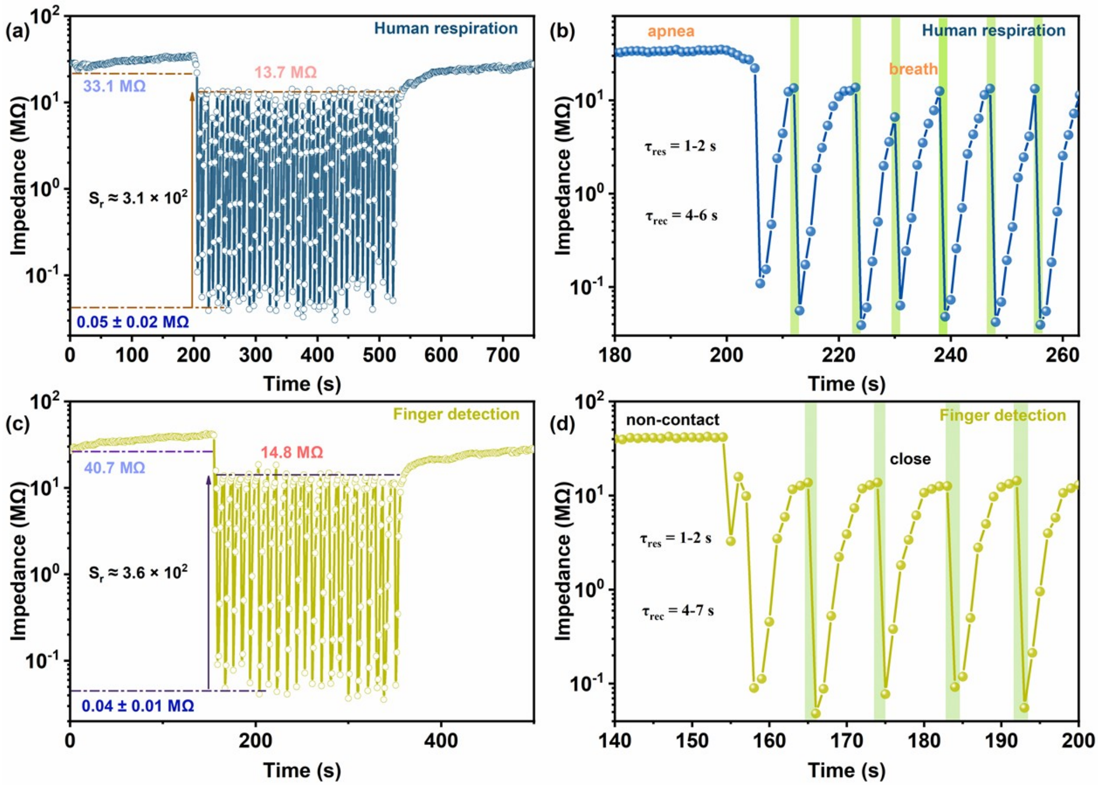

Fig. S9. The dynamic impedance and enlarged curves of monitoring (a, b) human respiration and (c, d) water evaporation from the finger using the Cs_2SnI_6 sensor.